

## Combined SM Higgs Limits at the Tevatron

N. Krumnack on behalf of the CDF and DØ collaborations

Iowa State University, Department of Physics and Astronomy, Physics Hall, Ames, IA 50011-3160, USA

We combine results from CDF and DØ on direct searches for a standard model (SM) Higgs boson ( $H$ ) in  $p\bar{p}$  collisions at the Fermilab Tevatron at  $\sqrt{s} = 1.96$  TeV. Compared to the previous Higgs Tevatron combination, more data and new channels ( $WH \rightarrow \tau\nu b\bar{b}$ ,  $VH \rightarrow \tau\tau b\bar{b}/jj\tau\tau$ ,  $VH \rightarrow jjb\bar{b}$ ,  $t\bar{t}H \rightarrow t\bar{t}b\bar{b}$ ) have been added. Most previously used channels have been reanalyzed to gain sensitivity. We use the latest parton distribution functions and  $gg \rightarrow H$  theoretical cross sections when comparing our limits to the SM predictions. With  $2.0\text{-}3.6 \text{ fb}^{-1}$  of data analyzed at CDF, and  $0.9\text{-}4.2 \text{ fb}^{-1}$  at DØ, the 95% C.L. upper limits on Higgs boson production are a factor of 2.5 (0.86) times the SM cross section for a Higgs boson mass of  $m_H = 115$  (165)  $\text{GeV}/c^2$ . Based on simulation, the corresponding median expected upper limits are 2.4 (1.1). The mass range excluded at 95% C.L. for a SM Higgs has been extended to  $160 < m_H < 170 \text{ GeV}/c^2$ .

### I. INTRODUCTION

The search for a mechanism for electroweak symmetry breaking, and in particular for a standard model (SM) Higgs boson has been a major goal of particle physics for many years, and is a central part of the Fermilab Tevatron physics program. Both the CDF and DØ experiments are reporting new combinations [2, 3] of multiple direct searches for the SM Higgs boson. The new searches include more data and improved analysis techniques compared to previous analyses. The sensitivities of these new combinations significantly exceed previous work [4, 5]. The most recent Tevatron Higgs combination [6] only included channels seeking Higgs bosons of masses between 155 and 200  $\text{GeV}/c^2$ , and the most recent combination over the entire mass range 100-200  $\text{GeV}/c^2$  was reported in April 2008 [7].

In this note, we combine the most recent results of all such searches in  $p\bar{p}$  collisions at  $\sqrt{s} = 1.96$  TeV. The analyses combined here seek signals of Higgs bosons produced in associated with vector bosons ( $q\bar{q} \rightarrow W/ZH$ ), through gluon-gluon fusion ( $gg \rightarrow H$ ), and through vector boson fusion (VBF) ( $q\bar{q} \rightarrow q'\bar{q}'H$ ) corresponding to integrated luminosities ranging from  $2.0\text{-}3.6 \text{ fb}^{-1}$  at CDF and  $0.9\text{-}4.2 \text{ fb}^{-1}$  at DØ. The Higgs boson decay modes studied are  $H \rightarrow b\bar{b}$ ,  $H \rightarrow W^+W^-$ ,  $H \rightarrow \tau^+\tau^-$  and  $H \rightarrow \gamma\gamma$ .

To simplify the combination, the searches are separated into 75 mutually exclusive final states (23 for CDF and 52 for DØ; see Table I and II) referred to as “analyses” in this note. The selection procedures for each analysis are detailed in Refs. [8] through [21], and are briefly described below.

### II. ACCEPTANCE, BACKGROUNDS AND LUMINOSITY

Event selections are similar for the corresponding CDF and DØ analyses. For the case of  $WH \rightarrow \ell\nu b\bar{b}$ , an isolated lepton ( $\ell = \text{electron or muon}$ ) and two jets

TABLE I: Luminosity, explored mass range and references for the different processes and final state ( $\ell = e, \mu$ ) for the CDF analyses

Channel	Lumi. ( $\text{fb}^{-1}$ )	$m_H$ range ( $\text{GeV}/c^2$ )	Ref.
$WH \rightarrow \ell\nu b\bar{b}$	2.7	100-150	[8]
$ZH \rightarrow \nu\bar{\nu} b\bar{b}$	2.1	105-150	[9]
$ZH \rightarrow \ell^+ \ell^- b\bar{b}$	2.7	100-150	[10]
$H \rightarrow W^+W^-$	3.6	110-200	[11]
$WH \rightarrow WW^+W^- \rightarrow \ell^\pm\nu\ell^\pm\nu$	3.6	110-200	[11]
$H + X \rightarrow \tau^+\tau^- + 2 \text{ jets}$	2.0	110-150	[12]
$WH + ZH \rightarrow jjb\bar{b}$	2.0	100-150	[13]

TABLE II: Luminosity, explored mass range and references for the different processes and final state ( $\ell = e, \mu$ ) for the DØ analyses

Channel	Lumi. ( $\text{fb}^{-1}$ )	$m_H$ range ( $\text{GeV}/c^2$ )	Ref.
$WH \rightarrow \ell\nu b\bar{b}$	2.7	100-150	[14]
$WH \rightarrow \tau\nu b\bar{b}$	0.9	105-145	[15]
$VH \rightarrow \tau\tau b\bar{b}/q\bar{q}\tau\tau$	1.0	105-145	[15]
$ZH \rightarrow \nu\bar{\nu} b\bar{b}$	2.1	105-145	[16]
$ZH \rightarrow \ell^+ \ell^- b\bar{b}$	2.3	105-145	[17]
$WH \rightarrow WW^+W^- \rightarrow \ell^\pm\nu\ell^\pm\nu$	1.1	120-200	[18]
$H \rightarrow W^+W^- \rightarrow \ell^\pm\nu\ell^\mp\nu$	3.0-4.2	115-200	[19]
$H \rightarrow \gamma\gamma$	4.2	100-150	[20]
$t\bar{t}H \rightarrow t\bar{t}b\bar{b}$	2.1	105-145	[21]

are required, with one or more  $b$ -tagged jet, i.e., identified as containing a weakly-decaying  $B$  hadron. Selected events must also display a significant imbalance in transverse momentum (referred to as missing transverse energy or  $\cancel{E}_T$ ). Events with more than one isolated lepton are vetoed. For the DØ  $WH \rightarrow \ell\nu b\bar{b}$  analyses, two and three jet events are analyzed separately,

and in each of these samples two non-overlapping  $b$ -tagged samples are defined, one being a single “tight”  $b$ -tag (ST) sample, and the other a double “loose”  $b$ -tag (DT) sample. The tight and loose  $b$ -tagging criteria are defined with respect to the mis-identification rate that the  $b$ -tagging algorithm yields for light quark or gluon jets (“mistag rate”) typically  $\leq 0.5\%$  or  $\leq 1.5\%$ , respectively. The final variable is a neural network output which takes as input seven kinematics variables and a matrix element discriminant for the 2 jet sample, while for the 3 jet sample the dijet invariant mass is used. In this combination, we add a new analysis  $WH \rightarrow \tau\nu b\bar{b}$  in which the  $\tau$  is identified through its hadronic decays. This analysis is sensitive to  $ZH \rightarrow \tau\cancel{E}_T b\bar{b}$  as well in those cases where a  $\tau$  fails to be identified. The analysis is carried out according to the type of reconstructed  $\tau$  and is also separated into two and three jets with DT events only. It uses the dijet invariant mass of the  $b\bar{b}$  system as discriminant variable.

For the CDF  $WH \rightarrow \ell\nu b\bar{b}$  analyses, the events are grouped into six categories. In addition to the selections requiring an identified lepton, events with an isolated track failing lepton selection requirements are grouped into their own categories. This provides some acceptance for single prong tau decays. Within the lepton categories there are three  $b$ -tagging categories – two tight  $b$ -tags (TDT), one tight  $b$ -tag and one loose  $b$ -tag (LDT), and a single, tight,  $b$ -tag (ST). In each category, two discriminants are calculated for each event. One neural network discriminant is trained at each  $m_H$  in the test range, separately for each category. A second discriminant is a boosted decision tree, featuring not only event kinematic and  $b$ -tagging observables, but matrix element discriminants as well. These two discriminants are then combined together using an evolutionary neural network [22] to form a single discriminant with optimal performance.

For the  $ZH \rightarrow \nu\bar{\nu} b\bar{b}$  analyses, the selection is similar to the  $WH$  selection, except all events with isolated leptons are vetoed and stronger multijet background suppression techniques are applied. Both CDF and DØ analyses use a track-based missing transverse momentum calculation as a discriminant against false  $\cancel{E}_T$ . There is a sizable fraction of  $WH \rightarrow \ell\nu b\bar{b}$  signal in which the lepton is undetected, that is selected in the  $ZH \rightarrow \nu\bar{\nu} b\bar{b}$  samples, so these analyses are also referred to as  $VH \rightarrow \cancel{E}_T b\bar{b}$ . The CDF analysis uses three non-overlapping samples of events (TDT, LDT and ST as for  $WH$ ) while DØ uses a sample of events having one tight  $b$ -tag jet and one loose  $b$ -tag jet. CDF used neural-network discriminants as the final variables, while DØ uses boosted decision trees as advanced analysis technique.

The  $ZH \rightarrow \ell^+\ell^- b\bar{b}$  analyses require two isolated leptons and at least two jets. They use non-overlapping samples of events with one tight  $b$ -tag and two loose  $b$ -tags. For the DØ analysis neural-

network and boosted decision trees discriminants are the final variables for setting limits (depending on the sub-channel), while CDF uses the output of a 2-dimensional neural-network. CDF corrects jet energies for  $\cancel{E}_T$  using a neural network approach. In this analysis also the events are divided into three tagging categories: tight double tags, loose double tags, and single tags.

For the  $H \rightarrow W^+W^-$  analyses, signal events are characterized by a large  $\cancel{E}_T$  and two opposite-signed, isolated leptons. The presence of neutrinos in the final state prevents the reconstruction of the candidate Higgs boson mass. DØ selects events containing electrons and muons, dividing the data sample into three final states:  $e^+e^-$ ,  $e^\pm\mu^\mp$ , and  $\mu^+\mu^-$ . CDF separates the  $H \rightarrow W^+W^-$  events in five non-overlapping samples, labeled “high  $s/b$ ” and “low  $s/b$ ” for the lepton selection categories, and also split by the number of jets: 0, 1, or 2+ jets. The sample with two or more jets is not split into low  $s/b$  and high  $s/b$  lepton categories. The division of events into jet categories allows the analysis discriminants to separate three different categories of signals from the backgrounds more effectively. The signal production mechanisms considered are  $gg \rightarrow H \rightarrow W^+W^-$ ,  $WH+ZH \rightarrow jjW^+W^-$ , and the vector-boson fusion process. The final discriminants are neural-network outputs for DØ and neural-network output including likelihoods constructed from matrix-element probabilities (ME) as input to the neural network, for CDF, in the 0-jet bin, else the ME are not used. All analyses in this channel have been updated with more data and analysis improvements.

The CDF collaboration also contributes an analysis searching for Higgs bosons decaying to a tau lepton pair, in three separate production channels: direct  $p\bar{p} \rightarrow H$  production, associated  $WH$  or  $ZH$  production, or vector boson production with  $H$  and forward jets in the final state. In this analysis, the final variable for setting limits is a combination of several neural-network discriminants.

DØ also contributes a new analysis for the final state  $\tau\tau$  jet jet, which is sensitive to the  $VH \rightarrow jj\tau\tau$ ,  $ZH \rightarrow \tau\tau b\bar{b}$ , VBF and gluon gluon fusion (with two additional jets) mechanisms. It uses a neural network output as discriminant variable.

The CDF collaboration introduces a new all-hadronic channel,  $WH+ZH \rightarrow jjb\bar{b}$  for this combination. Events are selected with four jets, at least two of which are  $b$ -tagged with the tight  $b$ -tagger. The large QCD backgrounds are estimated with the use of data control samples, and the final variable is a matrix element signal probability discriminant.

The DØ collaboration contributes three  $WH \rightarrow WW^+W^-$  analyses, where the associated  $W$  boson and the  $W$  boson from the Higgs boson decay which has the same charge are required to decay leptonically, thereby defining three like-sign dilepton final states ( $e^\pm e^\pm$ ,  $e^\pm\mu^\pm$ , and  $\mu^\pm\mu^\pm$ ) containing all decays of the

third  $W$  boson. In this analysis, which has not been updated for this combination, the final variable is a likelihood discriminant formed from several topological variables. CDF contributes a  $WH \rightarrow WW^+W^-$  analysis using a selection of like-sign dileptons and a neural network to further purify the signal.  $D\bar{O}$  also contributes an analysis searching for direct Higgs boson production decaying to a photon pair in  $4.2 \text{ fb}^{-1}$  of data. In this analysis, the final variable is the invariant mass of the two-photon system.

Another new search from  $D\bar{O}$  is included in this combination, namely the search for  $t\bar{t}H \rightarrow t\bar{t}b\bar{b}$ . Here the samples are analyzed independently according to the number of  $b$ -tagged jets (1,2,3, i.e. ST,DT,TT) and the total number of jets (4 or 5). The total transverse energy of the reconstructed objects ( $H_T$ ) is used as discriminant variable.

All Higgs boson signals are simulated using PYTHIA [23], and CTEQ5L or CTEQ6L [24] leading-order (LO) parton distribution functions. The  $gg \rightarrow H$  production cross section is calculated at NNLL in QCD and also includes two-loop electroweak effects; see Refs. [25, 26] and references therein for the different steps of these calculations. The newer calculation includes a more thorough treatment of higher-order radiative corrections, particularly those involving  $b$  quark loops. The  $gg \rightarrow H$  production cross section depends strongly on the PDF set chosen and the accompanying value of  $\alpha_s$ . The cross sections used here are calculated with the MSTW 2008 NNLO PDF set [30]. The new  $gg \rightarrow H$  cross sections supersede those used in the update of Summer 2008 [6, 27, 29], which had a simpler treatment of radiative corrections and used the older MRST 2002 PDF set [31]. The Higgs boson production cross sections used here are listed in [1] (originally from [26]). We include all significant Higgs production modes in the high mass search: besides gluon-gluon fusion through a virtual top quark loop ( $ggH$ ), we include production in association with a  $W$  or  $Z$  vector boson (VH) [28, 32, 33], and vector boson fusion (VBF) [28, 34].

The Higgs boson decay branching ratio predictions are calculated with HDECAY [35]. For both CDF and  $D\bar{O}$ , events from multijet (instrumental) backgrounds (“QCD production”) are measured in data with different methods, in orthogonal samples. For CDF, backgrounds from other SM processes were generated using PYTHIA, ALPGEN [36], MC@NLO [37] and HERWIG [38] programs. For  $D\bar{O}$ , these backgrounds were generated using PYTHIA, ALPGEN, and COMPHEP [39], with PYTHIA providing parton-showering and hadronization for all the generators. These background processes were normalized using either experimental data or next-to-leading order calculations (from MCFM [40] for  $W$ + heavy flavor process).

Integrated luminosities, and references to the collaborations’ public documentation for each analysis

are given in Table I for CDF and in Table II for  $D\bar{O}$ . The tables include the ranges of Higgs boson mass ( $m_H$ ) over which the searches were performed.

### III. DISTRIBUTIONS OF CANDIDATES

The number of channels combined is quite large, and the number of bins in each channel is large. Therefore, the task of assembling histograms and checking whether the expected and observed limits are consistent with the input predictions and observed data is difficult. We therefore provide histograms that aggregate all channels’ signal, background, and data together. In order to preserve most of the sensitivity gain that is achieved by the analyses by binning the data instead of collecting them all together and counting, we aggregate the data and predictions in narrow bins of signal-to-background ratio,  $s/b$ . Data with similar  $s/b$  may be added together with no loss in sensitivity, assuming similar systematic errors on the predictions. The aggregate histograms do not show the effects of systematic uncertainties, but instead compare the data with the central predictions supplied by each analysis.

The range of  $s/b$  is quite large in each analysis, and so  $\log_{10}(s/b)$  is chosen as the plotting variable. Plots of the distributions of  $\log_{10}(s/b)$  are shown for  $m_H = 115$  and  $165 \text{ GeV}/c^2$  in Figure 1. These distributions can be integrated from the high- $s/b$  side downwards, showing the sums of signal, background, and data for the most pure portions of the selection of all channels added together. These integrals can be seen in Figure 2.

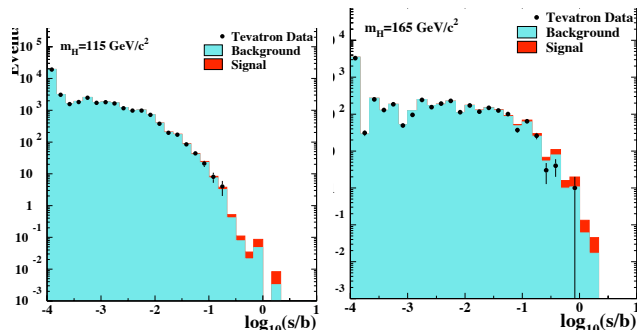


FIG. 1: Distributions of  $\log_{10}(s/b)$ , for the data from all contributing channels from CDF and  $D\bar{O}$ , for Higgs boson masses of 115 and  $165 \text{ GeV}/c^2$ . The data are shown with points, and the signal is shown stacked on top of the backgrounds. Underflows and overflows are collected into the bottom and top bins.

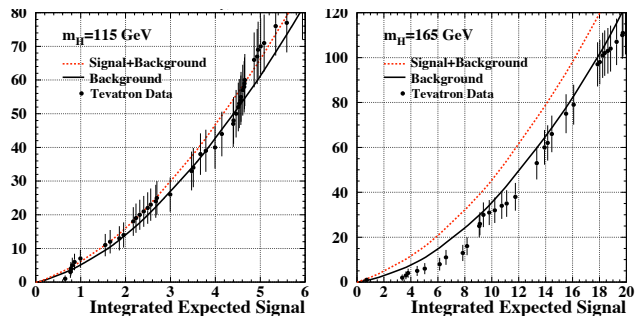


FIG. 2: Integrated distributions of  $s/b$ , starting at the high  $s/b$  side. The total signal+background and background-only integrals are shown separately, along with the data sums. Data are only shown for bins that have data events in them.

#### IV. COMBINING CHANNELS

To gain confidence that the final result does not depend on the details of the statistical formulation, we perform two types of combinations, using the Bayesian and Modified Frequentist approaches, which give similar results (within 10%). Both methods rely on distributions in the final discriminants, and not just on their single integrated values. Systematic uncertainties enter as uncertainties on the expected number of signal and background events, as well as on the distribution of the discriminants in each analysis (“shape uncertainties”). Both methods use likelihood calculations based on Poisson probabilities. Detailed descriptions of the techniques can be found in [1] as well as in [2] for the Bayesian Approach and in [3, 41, 42] for the Modified Frequentist Approach.

##### A. Systematic Uncertainties

Systematic uncertainties differ between experiments and analyses, and they affect the rates and shapes of the predicted signal and background in correlated ways. The combined results incorporate the sensitivity of predictions to values of nuisance parameters, and include correlations, between rates and shapes, between signals and backgrounds, and between channels within experiments and between experiments. More on these issues can be found in the individual analysis notes [8] through [21] and in the combination note [1].

#### V. COMBINED RESULTS

Using the combination procedures outlined in [1], we extract limits on SM Higgs boson production  $\sigma \times B(H \rightarrow X)$  in  $p\bar{p}$  collisions at  $\sqrt{s} = 1.96$  TeV for  $m_H = 100 - 200$  GeV/ $c^2$ . To facilitate comparisons

with the standard model and to accommodate analyses with different degrees of sensitivity, we present our results in terms of the ratio of obtained limits to cross section in the SM, as a function of Higgs boson mass, for test masses for which both experiments have performed dedicated searches in different channels. A value of the combined limit ratio which is less than or equal to one would indicate that that particular Higgs boson mass is excluded at the 95% C.L.

The combinations of results of each single experiment, as used in this Tevatron combination, yield the following ratios of 95% C.L. observed (expected) limits to the SM cross section: 3.6 (3.2) for CDF and 3.7 (3.9) for DØ at  $m_H = 115$  GeV/ $c^2$ , and 1.5 (1.6) for CDF and 1.3 (1.8) for DØ at  $m_H = 165$  GeV/ $c^2$ .

The ratios of the 95% C.L. expected and observed limit to the SM cross section are shown in Figure 3 for the combined CDF and DØ analyses. Tables with the observed and median expected ratios as obtained by the Bayesian and the  $CL_S$  methods are listed in [1]. In the following summary we quote only the limits obtained with the Bayesian method since they are slightly more conservative (based on the expected limits) for the quoted values, but all the equivalent numbers for the  $CL_S$  method can be retrieved from [1]. We obtain the observed (expected) values of 2.5 (2.4) at  $m_H = 115$  GeV/ $c^2$ , 0.99 (1.1) at  $m_H = 160$  GeV/ $c^2$ , 0.86 (1.1) at  $m_H = 165$  GeV/ $c^2$ , and 0.99 (1.4) at  $m_H = 170$  GeV/ $c^2$ . We exclude at the 95% C.L. the production of a standard model Higgs boson with mass between 160 and 170 GeV/ $c^2$ . This result is obtained with both Bayesian and  $CL_S$  calculations.

We also show in Figure 4 the 1- $CL_S$  distribution as a function of the Higgs boson mass, at high mass ( $\geq 150$  GeV/ $c^2$ ) which is directly interpreted as the level of exclusion at 95% C.L. of our search. Note that this figure is obtained using the  $CL_S$  method. The 90% C.L. line is also shown on the figure. We provide the Log-likelihood ratio (LLR) values for our combined Higgs boson search, as obtained using the  $CL_S$  method in [1].

In summary, we have combined all available CDF and DØ results on SM Higgs search, based on luminosities ranging from 0.9 to 4.2 fb $^{-1}$ . Compared to our previous combination, new channels have been added and most previously used channels have been reanalyzed to gain sensitivity. We use the latest parton distribution functions and  $gg \rightarrow H$  theoretical cross sections when comparing our limits to the SM predictions at high mass.

The 95% C.L. upper limits on Higgs boson production are a factor of 2.5 (0.86) times the SM cross section for a Higgs boson mass of  $m_H = 115$  (165) GeV/ $c^2$ . Based on simulation, the corresponding median expected upper limits are 2.4 (1.1). Standard Model branching ratios, calculated as functions of the Higgs boson mass, are assumed. These results extend significantly the individual limits

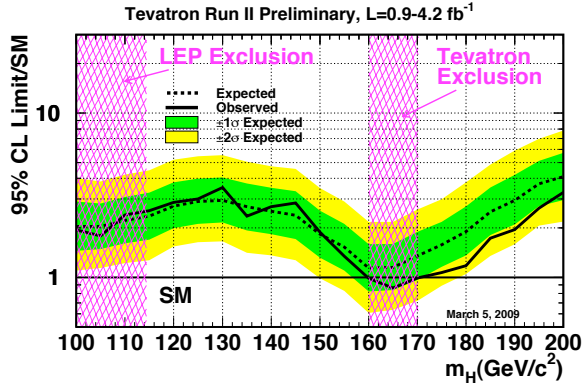


FIG. 3: Observed and expected (median, for the background-only hypothesis) 95% C.L. upper limits on the ratios to the SM cross section, as functions of the Higgs boson mass for the combined CDF and  $D\bar{O}$  analyses. The limits are expressed as a multiple of the SM prediction for test masses (every  $5 \text{ GeV}/c^2$ ) for which both experiments have performed dedicated searches in different channels. The points are joined by straight lines for better readability. The bands indicate the 68% and 95% probability regions where the limits can fluctuate, in the absence of signal. The limits displayed in this figure are obtained with the Bayesian calculation.

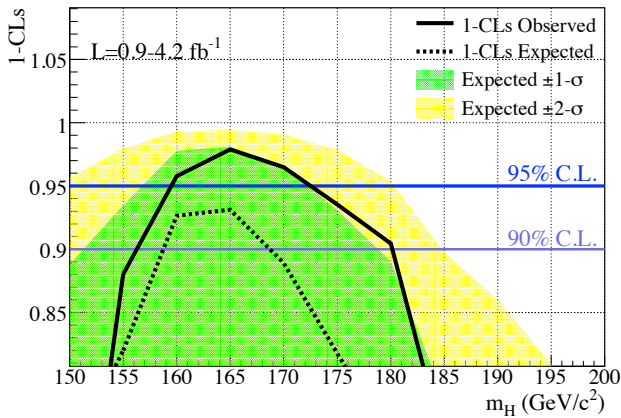


FIG. 4: Distributions of  $1-CL_S$  as a function of the Higgs boson mass (in steps of  $5 \text{ GeV}/c^2$ ), as obtained with  $CL_S$  method. for the combination of the CDF and  $D\bar{O}$  analyses.

of each collaboration and our previous combination. The mass range excluded at 95% C.L. for a SM Higgs has been extended to  $160 < m_H < 170 \text{ GeV}/c^2$ . The sensitivity of our combined search is expected to grow substantially in the near future with the additional luminosity already recorded at the Tevatron and not yet analyzed, and with additional improvements of our analysis techniques which will be propagated in the current and future analyses.

- [1] The TEVNPH Working Group, Combined CDF and  $D\bar{O}$  Upper Limits on Standard Model Higgs-Boson Production with up to  $4.2 \text{ fb}^{-1}$  of Data, FERMILAB-PUB-09-060-E, CDF Note 9713,  $D\bar{O}$  Note 5889 (2009).
- [2] CDF Collaboration, “Combined Upper Limit on Standard Model Higgs Boson Production for Winter 2009”, CDF Conference Note 9674 (2009).

- [3]  $D\bar{O}$  Collaboration, “Combined upper limits on standard model Higgs boson production from the  $D\bar{O}$  experiment with up to  $4.2 \text{ fb}^{-1}$  of data”  $D\bar{O}$  Conference Note 5896 (2009).
- [4] CDF Collaboration, “Combined Upper Limit on Standard Model Higgs Boson Production for Summer 2008”, CDF Conference Note 9502 (2008).
- [5]  $D\bar{O}$  Collaboration, “Combined upper limits on stan-

- standard model Higgs boson production from the  $D\bar{O}$  experiment in 1.1-3.0  $\text{fb}^{-1}$ ”  $D\bar{O}$  Conference Note 5756 (2008).
- [6] The CDF and  $D\bar{O}$  Collaborations and the TEVN-PHWG Working Group, “Combined CDF and  $D\bar{O}$  Upper Limits on Standard Model Higgs Boson Production at Higg Mass (155-200 GeV) with 3  $\text{fb}^{-1}$  of Data”, FERMILAB-PUB-08-270-E, CDF Note 9465,  $D\bar{O}$  Note 5754, arXiv:0808.0534v1 [hep-ex] (2008).
- [7] The CDF and  $D\bar{O}$  Collaborations and the TEVN-PHWG Working Group, “Combined CDF and  $D\bar{O}$  Upper Limits on Standard Model Higgs Boson Production with up to 2.4  $\text{fb}^{-1}$  of Data”, FERMILAB-PUB-08-069-E, CDF Note 9290,  $D\bar{O}$  Note 5645, arXiv:0804.3423v1 [hep-ex] (2008).
- [8] CDF Collaboration, “Search for a Higgs Boson Produced in Association with a  $W$  Boson in  $p\bar{p}$  Collisions at  $\sqrt{s} = 1.96$  TeV”, arXiv:0906.5613, Phys. Rev. Lett 103, 092002 (2009).
- [9] CDF Collaboration, “Search for the Standard Model Higgs Boson in the  $\cancel{E}_T$  Plus Jets Sample”, CDF Conference Note 9642 (2008).
- [10] CDF Collaboration, “A Search for  $ZH \rightarrow \ell^+ \ell^- b\bar{b}$  in 2.7  $\text{fb}^{-1}$  using a Neural Network Discriminant”, CDF Conference Note 9665 (2009).
- [11] CDF Collaboration, “Search for  $H \rightarrow WW^*$  Production Using 3.6  $\text{fb}^{-1}$  of Data”, CDF Conference Note 9500 (2009).
- [12] CDF Collaboration, “Search for SM Higgs using tau leptons using 2  $\text{fb}^{-1}$ ”, CDF Conference Note 9179.
- [13] CDF Collaboration, “A Search for the Standard Model Higgs Boson in the All-Hadronic channel using a Matrix Element Method”, CDF Conference Note 9366.
- [14]  $D\bar{O}$  Collaboration, “Search for WH associated production using a combined Neural Network and Matrix Element approach with 2.7  $\text{fb}^{-1}$  of Run II data,”  $D\bar{O}$  Conference Note 5828.
- [15]  $D\bar{O}$  Collaboration, “Search for the standard model Higgs boson in  $\tau$  final states”,  $D\bar{O}$  Conference note 5883.
- [16]  $D\bar{O}$  Collaboration, “Search for the standard model Higgs boson in the  $HZ \rightarrow b\bar{b}\nu\nu$  channel in 2.1  $\text{fb}^{-1}$  of  $p\bar{p}$  collisions at  $\sqrt{s} = 1.96$  TeV”,  $D\bar{O}$  Conference note 5586.
- [17]  $D\bar{O}$  Collaboration, “A Search for  $ZH \rightarrow \ell^+ \ell^- b\bar{b}$  Production at  $D\bar{O}$  in  $p\bar{p}$  Collisions at  $\sqrt{s} = 1.96$  TeV”,  $D\bar{O}$  Conference Note 5570.
- [18]  $D\bar{O}$  Collaboration, “Search for associated Higgs boson production  $WH \rightarrow WW^* \rightarrow \ell^\pm \nu \ell'^\pm \nu' + X$  in  $p\bar{p}$  collisions at  $\sqrt{s} = 1.96$  TeV”,  $D\bar{O}$  Conference Note 5485.
- [19]  $D\bar{O}$  Collaboration, “Search for Higgs production in dilepton plus missing energy final states with 3.0-4.2  $\text{fb}^{-1}$  of  $p\bar{p}$  collisions at  $\sqrt{s} = 1.96$  TeV”,  $D\bar{O}$  Conference Note 5871.
- [20]  $D\bar{O}$  Collaboration, “Search for the Standard Model Higgs boson in  $\gamma\gamma$  final state with 4.2  $\text{fb}^{-1}$  data”,  $D\bar{O}$  Conference Note 5858.
- [21]  $D\bar{O}$  Collaboration, “Search for the standard model Higgs boson in the  $t\bar{t}H \rightarrow t\bar{t}b\bar{b}$  channel”,  $D\bar{O}$  Conference note 5739.
- [22] K. O. Stanley and R. Miikkulainen, “Evolutionary Computation”, **10 (2)** 99-127 (2002); S. Whiteson and D. Whiteson, hep-ex/0607012 (2006).
- [23] T. Sjöstrand, L. Lonnblad and S. Mrenna, “PYTHIA 6.2: Physics and manual,” arXiv:hep-ph/0108264.
- [24] H. L. Lai *et al.*, “Improved Parton Distributions from Global Analysis of Recent Deep Inelastic Scattering and Inclusive Jet Data”, Phys. Rev D **55**, 1280 (1997).
- [25] C. Anastasiou, R. Boughezal and F. Petriello, “Mixed QCD-electroweak corrections to Higgs boson production in gluon fusion”, arXiv:0811.3458 [hep-ph] (2008).
- [26] D. de Florian and M. Grazzini, “Higgs production through gluon fusion: updated cross sections at the Tevatron and the LHC”, arXiv:0901.2427v1 [hep-ph] (2009).
- [27] S. Catani, D. de Florian, M. Grazzini and P. Nason, “Soft-gluon resummation for Higgs boson production at hadron colliders,” JHEP **0307**, 028 (2003) [arXiv:hep-ph/0306211].
- [28] K. A. Assamagan *et al.* [Higgs Working Group Collaboration], “The Higgs working group: Summary report 2003,” arXiv:hep-ph/0406152.
- [29] U. Aglietti, R. Bonciani, G. Degrassi, A. Vicini, “Two-loop electroweak corrections to Higgs production in proton-proton collisions”, arXiv:hep-ph/0610033v1 (2006).
- [30] A. D. Martin, W. J. Stirling, R. S. Thorne and G. Watt, “Parton distributions for the LHC”, arXiv:0901.0002 [hep-ph] (2009).
- [31] A. D. Martin, R. G. Roberts, W. J. Stirling and R. S. Thorne, Phys. Lett. B **531**, 216 (2002) [arXiv:hep-ph/0201127].
- [32] O. Brein, A. Djouadi, and R. Harlander, “NNLO QCD corrections to the Higgs-strahlung processes at hadron colliders”, Phys. Lett. B **579**, 2004, 149-156.
- [33] Ciccolini, M. L. and Dittmaier, S. and Kramer, M., “Electroweak radiative corrections to associated WH and Z H production at hadron colliders”, Phys. Rev. D **68** (2003) 073003.
- [34] E. Berger and J. Campbell. “Higgs boson production in weak boson fusion at next-to-leading order”, Phys. Rev. D **70** (2004) 073011,
- [35] A. Djouadi, J. Kalinowski and M. Spira, “HDECAY: A program for Higgs boson decays in the standard model and its supersymmetric extension,” Comput. Phys. Commun. **108**, 56 (1998) [arXiv:hep-ph/9704448].
- [36] M. L. Mangano, M. Moretti, F. Piccinini, R. Pittau and A. D. Polosa, “ALPGEN, a generator for hard multiparton processes in hadronic collisions,” JHEP **0307**, 001 (2003) [arXiv:hep-ph/0206293].
- [37] S. Frixione and B.R. Webber, JHEP **06**, 029 (2002) [arXiv:hep-ph/0204244]
- [38] G. Corcella *et al.*, “HERWIG 6: An event generator for hadron emission reactions with interfering gluons (including supersymmetric processes),” JHEP **0101**, 010 (2001) [arXiv:hep-ph/0011363].
- [39] A. Pukhov *et al.*, “CompHEP: A package for evaluation of Feynman diagrams and integration over multiparticle phase space. User’s manual for version 33,” [arXiv:hep-ph/9908288].
- [40] J. Campbell and R. K. Ellis, <http://mcfm.fnal.gov/>.

- [41] T. Junk, Nucl. Instrum. Meth. A434, p. 435-443, 1999, A.L. Read, “Modified frequentist analysis of search results (the  $CL_s$  method)”, in F. James, L. Lyons and Y. Perrin (eds.), *Workshop on Confidence Limits*, CERN, Yellow Report 2000-005, available through [cdsweb.cern.ch](http://cdsweb.cern.ch).
- [42] W. Fisher, “Systematics and Limit Calculations,” FERMILAB-TM-2386-E.